



Discussion of sound propagation through the turbulent Martian atmosphere and implications for inference of turbulence spectra

Vladimir E. Ostashev,^{1,a)}  D. Keith Wilson,¹  Carl R. Hart,¹  Baptiste Chide,²  and Philippe Blanc-Benon³ 

¹United States Army Engineer Research and Development Center, 72 Lyme Road, Hanover, New Hampshire 03755, USA

²Institut de Recherche en Astrophysique et Planétologie, Toulouse, France

³Laboratoire de Mécanique des Fluides et d'Acoustique, Centre National de la Recherche Scientifique, Ecole Centrale de Lyon, Institut National des sciences appliquées Lyon, Université Lyon 1, Ecully, France

ABSTRACT:

Chide *et al.* [J. Acoust. Soc. Am. **155**, 420–435 (2024)] provide a first attempt to infer the spectrum of temperature fluctuations on Mars from experimental data on the variances of travel-time and log-amplitude fluctuations recorded by the microphone on board the Perseverance rover. However, the theoretical formulations that were used to interpret the travel-time data have limitations. In addition to explaining those issues, this article also outlines approaches for predicting statistical characteristics of acoustic signals in the Martian atmosphere. In particular, the experimentally observed dependence of the travel-time variance on the propagation range can be attributed to ground-blocking of buoyantly produced turbulent velocity fluctuations and the non-Markov character of phase fluctuations.

<https://doi.org/10.1121/10.0028166>

(Received 16 April 2024; revised 14 June 2024; accepted 13 July 2024; published online 16 August 2024)

[Editor: Andi Petculescu]

Pages: 1165–1170

I. INTRODUCTION

Chide *et al.*¹ provide experimental data on the travel-time statistics and log-amplitude variance for line-of-sight sound propagation obtained with the SuperCam microphone on board the Perseverance rover on Mars. The sound signals were generated by the SuperCam pulsed laser, which vaporized a small portion of the Martian surface. Using the experimental data, for the first time, Chide *et al.*¹ attempted to infer the spectrum of temperature fluctuations on Mars and its key parameters, such as the variance and length scale of fluctuations, and the slope of the spectrum. Three possible spectral models are considered: Gaussian, Kolmogorov, and generalized von Kármán. Using results from Iooss *et al.*² for the travel-time variance, Chide *et al.*¹ inferred the variance and outer length of temperature fluctuations for the Gaussian and generalized von Kármán spectra. Then, from the range dependence of the log-amplitude variance, they argue that the best agreement between theoretical predictions and experimental data is obtained with the generalized von Kármán spectrum with the slope parameter $p = -1/6$.

The experimental data in Chide *et al.*¹ are the first of their kind. However, the results by Iooss *et al.*² have limitations and should be cautiously used in predicting the travel-time fluctuations in the Martian atmosphere. Specifically, the travel-time variance in Iooss *et al.*² accounts for some terms of order ε^4 (ε is proportional to the refractive index fluctuation) but neglects other terms of the same order. It is also inconsistent with some results from the literature.³

Moreover, as noted in Chide *et al.*,¹ when inferring the temperature spectrum and its parameters, a simplifying assumption is made that wind velocity fluctuations can be ignored in predicting the travel-time and log-amplitude variances. For turbulence in the Earth atmosphere, the shear- and buoyancy-produced velocity fluctuations are the main factors driving fluctuations in acoustic signals during the daytime, whereas temperature fluctuations have a much lesser impact for most meteorological conditions, e.g., see Refs. 4–7. Although much less dense, the near-surface Martian atmosphere still resembles the Earth atmosphere^{8,9} such that a similar effect can be expected on Mars.

The goals of the current article are to discuss limitations in the results by Iooss *et al.*,² how these results are implemented in Chide *et al.*,¹ and the assumption of a motionless medium in predicting sound propagation in a turbulent atmosphere on Mars. We will also outline possible approaches for incorporating wind velocity fluctuations in such predictions.

The remainder of this article is organized as follows. Limitations in the results by Iooss *et al.*² are considered in Sec. II. Section III explains how these limitations affect reconstruction of the temperature spectrum in Chide *et al.*¹ Section IV presents approaches for incorporating wind velocity fluctuations into sound propagation models on Mars. Conclusions are presented in Sec. V.

II. THE MODEL BY IOOSS *et al.* (REF. 2)

This section outlines the results by Iooss *et al.*² and explains limitations in some of these results.

^{a)}Email: vladimir.ostashev@colorado.edu

Iooss *et al.*² study the statistics of the travel time t of sound propagation between a source and receiver in a random motionless medium. The travel time t is expressed as a perturbation series in which

$$t = t_0 + t_1 + t_2 + t_3 + t_4 + \dots \quad (1)$$

Here, t_0 is the travel time in a medium without random inhomogeneities; $t_1 \sim \varepsilon^1$, $t_2 \sim \varepsilon^2$, $t_3 \sim \varepsilon^3$, $t_4 \sim \varepsilon^4$, and so on; and a small parameter ε is the deviation of the refractive index squared from unity. In Eq. (1), t_1 and t_2 are calculated using the geometrical acoustics approximation. Then, omitting the higher order terms (such as t_3 and t_4), the mean travel time $\langle t \rangle$ and the travel-time variance σ_t^2 are obtained [see Eqs. (11)–(15) in Ref. 2] as follows:

$$\langle t \rangle = \frac{x}{c_0} + \frac{A_2 \sigma_\varepsilon^2 x^2}{24 c_0 L}, \quad (2)$$

$$\sigma_t^2 = \sigma_{t_1}^2 + \sigma_{t_2}^2 = \frac{A_1 \sigma_\varepsilon^2 L x}{2 c_0^2} + \frac{A_2^2 \sigma_\varepsilon^4 x^4}{288 c_0^2 L^2}. \quad (3)$$

Here, x is the distance between the source and receiver, c_0 is the sound speed in a medium without random inhomogeneities, σ_ε^2 and L are the variance and length scale, respectively, of the random field ε , and $\sigma_{t_1}^2$ and $\sigma_{t_2}^2$ are the travel-time variances corresponding to the second (t_1) and third (t_2) terms, respectively, in the perturbations series [Eq. (1)]. The numerical coefficients A_1 and A_2 depend on the spectrum $\Phi_\varepsilon(\kappa)$ of the random field ε .

For the generalized von Kármán spectrum of temperature fluctuations, Eq. (B6) in Chide *et al.*¹ provides the coefficients A_1 and A_2 such that

$$A_1 = \frac{\sqrt{\pi} \Gamma(p + 1/2)}{\Gamma(p)}, \quad A_2 = -\frac{\sqrt{\pi} \Gamma(p - 1/2)}{2\Gamma(p)}. \quad (4)$$

(Chide *et al.*¹ indicate that Iooss *et al.*² had a typo for A_2 .) In Eq. (4), Γ is the gamma function, and p is a parameter determining the slope of the generalized von Kármán spectrum in the inertial subrange of turbulence. This spectrum is defined as

$$\Phi_\varepsilon(\kappa) = \frac{\Gamma(p + 3/2)}{\pi^{3/2} \Gamma(p)} \frac{\sigma_\varepsilon^2 L^3}{(1 + \kappa^2 L^2)^{p+3/2}}. \quad (5)$$

Note that the (ordinary) von Kármán temperature spectrum [e.g., Eq. (6.26) in Ref. 4] corresponds to $p = 1/3$. References 1 and 2 provide only the dependence of $\Phi_\varepsilon(\kappa)$ on κ while not presenting the numerical coefficient and parameter $\sigma_\varepsilon^2 L^3$ in the right side of Eq. (5). These quantities can be uniquely determined using a formula expressing σ_ε^2 in terms of $\Phi_\varepsilon(\kappa)$ [e.g., Eq. (6.19) in Ref. 4]:

$$\sigma_\varepsilon^2 = 4\pi \int_0^\infty \Phi_\varepsilon(\kappa) \kappa^2 d\kappa. \quad (6)$$

Equation (5) coincides with Eq. (10) in Ref. 10, where the generalized von Kármán spectrum was also considered.

Reference 10 indicates that Eq. (5) is valid only for $p > 0$; otherwise, the integral in Eq. (6) diverges.

Equations (2) and (3) are the starting point of the analysis of the travel-time statistics on Mars.¹ In the remainder of this section, we analyze these equations and explain their limitations. The first terms on the right sides of Eqs. (2) and (3) are well-known results in wave propagation in random media.^{4,11–16} The second term in Eq. (2) has also been studied, e.g., see Refs. 11 and 17–20 and references therein. Using Eq. (2), the phase velocity v_{ph} of a sound wave in a random medium can be calculated as

$$v_{\text{ph}} = \frac{x}{\langle t \rangle} = c_0 \left(1 + \frac{A_2 \sigma_\varepsilon^2 x}{24 L} \right)^{-1}. \quad (7)$$

It follows from Eq. (7) that the random medium changes the phase velocity. This effect is termed the *velocity shift*. According to the references mentioned above, $v_{\text{ph}} > c_0$. This result is explained by Fermat's principle (which is applicable in the considered high-frequency approximation) and is also mentioned in Refs. 1 and 2: in deterministic and randomly inhomogeneous media, a wave propagates along the path that requires the least time. Equation (7) is consistent with Fermat's principle if $A_2 < 0$. It follows from Eq. (4) that $A_2 < 0$ if $p > 1/2$ in the generalized von Kármán spectrum. Note that Iooss *et al.*² indicate that A_2 is defined for $p > 1/2$.

However, if $0 < p < 1/2$, the coefficient A_2 becomes positive, thus, violating Fermat's principle. Therefore, $p > 1/2$ is the range of applicability of geometrical acoustics for calculating $\langle t \rangle$ and v_{ph} . This limitation can be overcome by calculating these quantities using the Rytov method, which generalizes geometrical acoustics by accounting for diffraction. The result is [e.g., see Eq. (25) in Shapiro *et al.*,¹⁸ where the last term in square brackets should be omitted in the considered high-frequency approximation]

$$v_{\text{ph}} = c_0 \left[1 - 4\pi^2 k_0^2 \int_0^\infty \Phi_\varepsilon(\kappa) \sin^2 \left(\frac{\kappa^2 x}{2k_0} \right) \frac{d\kappa}{\kappa x} \right]^{-1}. \quad (8)$$

Here, k_0 is the sound wavenumber in a medium without random inhomogeneities. Because the spectrum $\Phi_\varepsilon(\kappa)$ is always positive, the expression in the square brackets in Eq. (8) is less than one so that $v_{\text{ph}} > c_0$. Equation (8) can be used to calculate v_{ph} when geometrical acoustics is no longer applicable, e.g., if $0 < p < 1/2$ in the generalized von Kármán spectrum. [Note that Eq. (8) is valid for a plane sound wave, in which case the coefficient 24 in Eq. (7) should be replaced with 8, as follows from Eq. (12) in Ref. 2.]

Next, we point out that there are two difficulties with the second term in Eq. (3). First, in the asymptotic series, Eq. (1), Iooss *et al.*² retain terms of order ε^2 and omit higher order terms such as ε^4 . (Note that terms of order ε and ε^3 vanish after averaging.) This approximation should be consistently used in the subsequent derivations. Consequently,

the second term in Eq. (3) should be omitted because it is of order ε^4 .

The travel-time variance can be calculated to order ε^4 . To this end, the first five terms in Eq. (1) should be retained; that is,

$$\sigma_t^2 = \langle (t_0 + t_1 + t_2 + t_3 + t_4)^2 \rangle - \langle t_0 + t_1 + t_2 + t_3 + t_4 \rangle^2 + O(\varepsilon^6). \quad (9)$$

Here, keeping terms of order ε^4 and omitting higher order terms yields

$$\sigma_t^2 = \sigma_{t_1}^2 + \sigma_{t_2}^2 + 2\langle t_1 t_3 \rangle + O(\varepsilon^6). \quad (10)$$

This result differs from Eq. (3) obtained by Iooss *et al.*² by the term $2\langle t_1 t_3 \rangle$. This term should be taken into account if the travel-time variance is calculated to order ε^4 .

Second, the phase ϕ of a sound wave can be expressed in terms of the travel time: $\phi = \omega t$, where ω is the acoustic frequency. Therefore, the statistics of the travel-time fluctuations coincide with the phase fluctuations. The phase variance of a plane sound wave was obtained in Ref. 3 as a sum of two terms proportional to x and x^4 , i.e., the terms similar to those in Eq. (3); see Eq. (2.10) in Ref. 3. However, in the latter reference, the term proportional to x^4 is always negative while the second term in Eq. (3) is always positive. Reference 3 provides a physical explanation as to why the term proportional to x^4 is negative and substantiates the conclusion by an example of wave propagation through a random phase screen.

Finally, it should be noted that the second term in Eq. (2) should be much smaller compared to the first term. This is because Eq. (1) is an asymptotic series; if the third term t_2 has the same order as the second term t_1 , then all terms in the series should be taken into account. For example, Shapiro *et al.*¹⁸ show that the relative difference between v_{ph} and c_0 is less than 2%. Tatarskii¹⁷ uses the second Rytov approximation [which is similar to t_2 in Eq. (1)] to study the ranges of applicability of the first Rytov approximation (which is similar to t_1). Chide *et al.*¹ show that the second term in Eq. (2) is much smaller than the first term for experimental data from Mars.

The same conclusion applies to Eq. (3); i.e., the second term $\sigma_{t_2}^2$ in this equation should be much smaller than the first term $\sigma_{t_1}^2$. Iooss *et al.*² specifically state that Eq. (3) is valid when the travel-time variance is only weakly nonlinear.

III. INFERENCE OF TEMPERATURE SPECTRUM IN CHIDE *et al.* (REF. 1)

From the measurements of the mean travel time $\langle t \rangle$ on Mars, Chide *et al.*¹ showed that $v_{ph} > c_0$ in accordance with Fermat's principle. However, due to a small difference between v_{ph} and c_0 , it was not possible to infer the turbulence parameters.

Using the travel-time variance formulated in Iooss *et al.*² [i.e., Eq. (3)], Chide *et al.*¹ infer the variance σ_ε^2 and length scale L pertinent to temperature fluctuations. For the generalized von Kármán spectrum with $p = -1/6$, they obtain $\sigma_\varepsilon^2 = 2 \times 10^{-3}$ and $L = 11$ cm, whereas for the Gaussian spectrum, $\sigma_\varepsilon^2 = 7.4 \times 10^{-4}$ and $L = 14$ cm. It seems worthwhile to revisit these results because they are based on Iooss *et al.*² formulations, which have limitations.

First, it follows from Eq. (5) that for the generalized von Kármán spectral model with $p = -1/6$, the spectrum $\Phi_\varepsilon(\kappa) < 0$. This is a nonphysical result as $\Phi_\varepsilon(\kappa)$ should be positive. In other words, for this spectrum, the variance σ_ε^2 of a random field ε cannot be determined because the integral in Eq. (6) diverges.

The difficulty with the generalized von Kármán spectrum with $p = -1/6$ can be demonstrated from a different perspective. It follows from Eq. (4) that for $p = -1/6$, the coefficient $A_1 < 0$. This implies that the first term in the travel-time variance σ_t^2 [Eq. (3)] is negative, which is also nonphysical. In summary, the generalized von Kármán spectrum with $p = -1/6$ provides nonphysical results for the travel-time variance [Eq. (3)] and cannot be used to infer the variance σ_ε^2 and length scale L .

For the Gaussian spectrum, the variance and length scale can always be determined. However, for $\sigma_\varepsilon^2 = 7.4 \times 10^{-4}$, $L = 14$ cm and the propagation range x from 2.2 to 7.7 m as in the experiment on Mars,¹ the second term in Eq. (3) can become comparable to or even greater than the first term. Specifically, for $x = 2.2, 5,$ and 7.7 m, the ratios of these terms $\sigma_{t_2}^2/\sigma_{t_1}^2 = 0.04, 0.47,$ and 1.71 , respectively. This seems to violate the ranges of applicability of Eq. (3). Similar to Shapiro *et al.*,¹⁸ it is expected that the ratio $\sigma_{t_2}^2/\sigma_{t_1}^2$ should not exceed the value of about 0.02. Therefore, it is desirable to study the ranges of applicability of Eq. (3) in more detail before applying it.

Limitations of Eq. (3) in predicting the dependence of the travel-time variance σ_t^2 on range x are also evident from experimental data on Mars depicted as red diamonds in Fig. 1. The data correspond to σ_t^2 , which is measured during daytime and averaged over about one Martian year. It follows from Fig. 1 that σ_t^2 significantly deviates from the linear dependence on x , whereas Eq. (3) can only be used for small variations from the linear dependence.

In Chide *et al.*,¹ the slope of the temperature spectrum is determined from the dependence of log-amplitude variance σ_χ^2 on x , which is well-known in the literature. The best agreement between theoretical results for σ_χ^2 and experimental data is obtained for the generalized von Kármán temperature spectrum, Eq. (5), with $p = -1/6$. However, strictly speaking, this spectrum is nonphysical. This difficulty can be overcome with an approach suggested in Sec. IV.

IV. PREDICTING SOUND PROPAGATION IN A TURBULENT ATMOSPHERE ON MARS

Sound propagation through turbulence in the Earth atmosphere has been relatively well studied theoretically

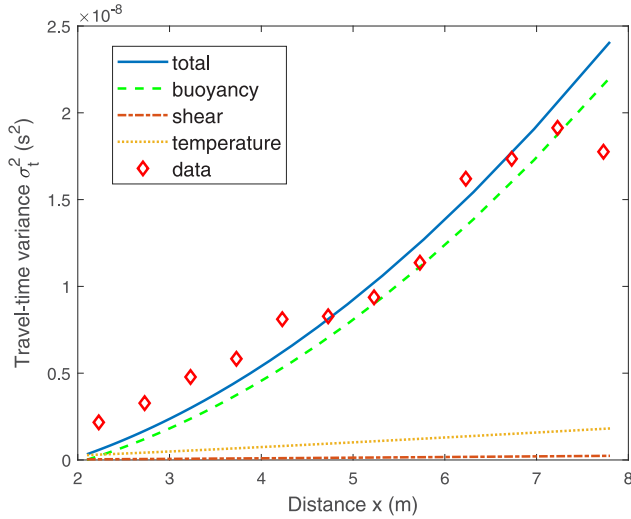


FIG. 1. (Color online) Travel-time variance σ_t^2 versus propagation range x . Red diamonds are experimental data from Fig. 4 in Chide *et al.* (Ref. 1). Solid line is the theoretical prediction for σ_t^2 based on Ref. 21. Dotted, dashed-dotted, and dashed lines are contributions to σ_t^2 due to temperature fluctuations and shear- and buoyancy-produced velocity fluctuations.

and experimentally, e.g., see Refs. 4 and 21–24 and references therein. Statistical moments of sound signals are expressed in terms of temperature fluctuations and shear- and buoyancy-produced velocity fluctuations. Because atmospheric turbulence on Earth and Mars has many similarities,^{8,9} we suggest that with some modifications, the theory of sound propagation in a turbulent atmosphere on Earth can also be used on Mars.

References 4 and 23 provide the log-amplitude variance for the ground-based source and elevated receiver, calculated in the Rytov method and Markov approximation, such that

$$\sigma_\chi^2 = \frac{\pi^2 k_0^2 x}{2} \int_0^1 d\eta \int_0^\infty \Phi_{\text{eff}}(\eta h; \kappa) \times \left[1 - \cos\left(\frac{\eta(1-\eta)\kappa^2 x}{k_0}\right) \right] \kappa d\kappa. \quad (11)$$

Here, h is the receiver height and $\Phi_{\text{eff}}(z; \kappa)$ is the effective spectrum of turbulence, the parameters of which can depend on the height z above the ground. For the generalized von Kármán spectral model, $\Phi_{\text{eff}}(z; \kappa)$ can be written as^{4,5}

$$\Phi_{\text{eff}}(z; \kappa) = \frac{\Gamma(\alpha)}{\pi^{3/2} \Gamma(\alpha - 3/2)} \left[\frac{\sigma_T^2(z) L_T^3(z)}{T_0^2 (1 + \kappa^2 L_T^2(z))^\alpha} + \frac{4\alpha \sigma_{v,s}^2 L_{v,s}^5(z) \kappa^2}{c_0^2 (1 + \kappa^2 L_{v,s}^2(z))^{\alpha+1}} + \frac{4\alpha \sigma_{v,b}^2 L_{v,b}^5(z) \kappa^2}{c_0^2 (1 + \kappa^2 L_{v,b}^2(z))^{\alpha+1}} \right]. \quad (12)$$

Here, α is a parameter; T_0 is the reference temperature; σ_T^2 , $\sigma_{v,s}^2$, and $\sigma_{v,b}^2$ are the variances of temperature fluctuations and shear- and buoyancy-produced velocity fluctuations,

respectively; and L_T , $L_{v,s}$, and $L_{v,b}$ are the length scales of the corresponding fluctuations. The ordinary von Kármán spectrum corresponds to $\alpha = 11/6$ in Eq. (12). In a neutral or convective planetary boundary layer (PBL), using the Monin-Obukhov and mixed-layer similarity theories, the variances σ_T^2 , $\sigma_{v,s}^2$, $\sigma_{v,b}^2$ and length scales L_T , $L_{v,s}$, $L_{v,b}$ in Eq. (12) can be expressed in terms of the meteorological parameters:^{4,21} the air temperature near the ground T_s , the friction velocity u_* , the sensible heat flux from the surface to the air Q_H , and the PBL inversion height z_i . Some of the variances and length scales depend on the height z above the ground while others do not. Note that Chide *et al.*¹ use a similar equation for σ_χ^2 except that the effective spectrum Φ_{eff} does not include velocity fluctuations and does not depend on z .

Equations (11) and (12), where $\alpha = 11/6$, predict the log-amplitude variance σ_χ^2 in the PBL on Earth with a relatively good agreement between theoretical results and experimental data.²³ With some modifications, Eqs. (11) and (12) can also be used to predict σ_χ^2 on Mars. First, as the spectra of temperature and wind velocity fluctuations might be flatter on Mars than on Earth,^{1,25} it is reasonable to assume that α can deviate from 11/6, as was already done in Ref. 1 for temperature fluctuations.

Second, the log-amplitude variance σ_χ^2 is affected by small-scale inhomogeneities of the order of the first Fresnel zone. Such small inhomogeneities are likely in the inertial subrange of turbulence, where $\kappa L_T \gg 1$, $\kappa L_{v,s} \gg 1$, and $\kappa L_{v,b} \gg 1$ in Eq. (12). In this case, the effective turbulence spectrum, Eq. (12), simplifies to

$$\Phi_{\text{eff}}(z; \kappa) = Q C_{\text{eff}}^2(z) \kappa^{-2\alpha}. \quad (13)$$

Here, $Q = \Gamma(\alpha)/(\pi^{3/2} \Gamma(\alpha - 3/2))$ is a numerical coefficient, and C_{eff}^2 is a parameter given by

$$C_{\text{eff}}^2(z) = \frac{\sigma_T^2(z) L_T^{3-2\alpha}(z)}{T_0^2} + \frac{4\alpha \sigma_{v,s}^2 L_{v,s}^{3-2\alpha}(z)}{c_0^2} + \frac{4\alpha \sigma_{v,b}^2 L_{v,b}^{3-2\alpha}(z)}{c_0^2}. \quad (14)$$

For the ordinary von Kármán spectrum ($\alpha = 11/6$), Eqs. (13) and (14) coincide with Eq. (7.31) in Ref. 4, where C_{eff}^2 is termed as the effective structure function parameter of temperature and wind velocity fluctuations, which determines the intensity of turbulence in the inertial subrange.

With these results, comparison of theoretical predictions for the log-amplitude variance based on Eqs. (11) and (13) with experimental data on Mars can yield the slope of the effective spectrum and intensity of turbulence in the inertial subrange. Note that in the inertial subrange, the generalized von Kármán spectrum $\Phi_\varepsilon(\kappa)$ [Eq. (5)] is also proportional to $\kappa^{-2\alpha}$, where $\alpha = p + 3/2$. However, this spectrum becomes nonphysical for $p = -1/6$, whereas the spectrum given by Eq. (13) can still be used in this case.

Next, we consider the travel-time variance σ_t^2 , which can be expressed in terms of the variance of phase

fluctuations σ_ϕ^2 using a formula $\sigma_t^2 = \sigma_\phi^2/\omega^2$. In contrast to the log-amplitude variance, phase fluctuations are affected by the largest turbulence eddies. By accounting for ground-blocking of buoyancy-produced velocity fluctuations²⁶ and non-Markov character of phase fluctuations, Ref. 21 provides the latest theory for the phase variance σ_ϕ^2 of acoustic signals in a daytime PBL on Earth and verifies the results by comparing them to experimental data. The isotropic part of turbulence is modeled with the ordinary von Kármán spectra of temperature fluctuations and shear- and buoyancy-produced velocity fluctuations appearing in the right side of Eq. (12).

With some modifications, the results from Ref. 21 can be used to explain the nonlinear range dependence of the travel-time variance in Fig. 1. To this end, the parameters pertinent to Earth should be replaced with those on Mars. Because the experimental data in Fig. 1 correspond to σ_t^2 , which is averaged over one Martian year, we use the mean temperature $T_0 = T_s = 242$ K and sound speed $c_0 = 255$ m/s reported in Chide *et al.*¹ The friction velocity u_* , sensible heat flux $Q_H = T_*\rho_a C_P u_*$ (where T_* is the temperature scale), and PBL inversion height z_i were not measured during the Perseverance mission. To roughly estimate these meteorological parameters, the mean values of the friction velocity and temperature scale suggested in Ref. 8 are used: $u_* = 0.4$ m/s and $T_* = 1$ K. With these parameters, we have for the mean heat flux $Q_H = 4.38$ W/m². From the Mars Climate Database version 6.1,²⁷ the PBL height averaged over a year during hours 10:00–14:00 can be estimated as $z_i = 4$ km. Furthermore, on Mars, the gravitational acceleration is $g = 3.7$ m/s², air density is $\rho_a = 0.015$ kg/m³, specific heat at constant pressure is $C_P = 730$ J/(K kg), and von Kármán constant is $\kappa_v = 0.4$.⁸

Given these parameters, the source and receiver geometry in Chide *et al.*,¹ and formulations in Ref. 21, the travel-time variance can be calculated. The results are presented in Fig. 1, where the surface heat flux $Q_H = 1.05$ W/m² is used as an adjustable parameter, and other parameters are specified above. In Fig. 1, the solid line is the theoretical prediction for the travel-time variance σ_t^2 , while the dotted, dashed-dotted, and dashed lines are contributions to σ_t^2 that result from temperature fluctuations and shear- and buoyancy-produced velocity fluctuations, respectively. It follows from Fig. 1 that the buoyancy-produced velocity fluctuations are the largest contribution to σ_t^2 , whereas the temperature fluctuations and shear-produced velocity fluctuations have much lesser impact. This conclusion remains the same for $Q_H = 4.38$ W/m² and is due to the fact that, on average, the buoyancy-produced velocity fluctuations are probably the largest, most energetic turbulence eddies during daytime on Mars. A similar result has been obtained for most meteorological conditions on Earth.^{5–7}

It follows from the experimental setup on Mars¹ that in Fig. 1, increasing range x corresponds to increasing angle θ between the direction of sound propagation and vertical. Ground-blocking of buoyancy-produced velocity fluctuations diminishes fluctuations in the vertical direction

($\theta = 0$); these fluctuations increase as the angle θ increases. As a result, the travel-time variance σ_t^2 in Fig. 1 increases faster with range than the linear dependence ($\sigma_t^2 \sim x$), thus, enabling to explain the range dependence of the experimental data, at least qualitatively.

It should be noted that the mean values of u_* , T_* , and z_i , pertinent for the experimental data in Fig. 1, likely differ from those in Refs. 8 and 27. Also, the generalized von Kármán temperature and velocity spectra should probably be used on Mars rather than the ordinary von Kármán spectra employed in Ref. 21. Therefore, Fig. 1 should be considered as a starting point in comparing theoretical predictions for the travel-time variance with experimental data on Mars rather than a final result.

V. CONCLUSIONS

This article explained difficulties in formulations for the travel-time variance by Iooss *et al.*² Limitations in applying these formulations to sound propagation through turbulence in the Martian atmosphere¹ were highlighted. Furthermore, it was argued that wind velocity fluctuations are the main factor driving fluctuations of acoustic signals during daytime on Earth^{4–7} and, most probably, on Mars. Approaches were suggested for predicting sound propagation through turbulence on Mars and inferring turbulence spectra. In particular, by accounting for ground-blocking of buoyancy-produced velocity fluctuations and the non-Markov character of phase fluctuations, it was possible to explain, at least qualitatively, the range dependence of the travel-time variance on Mars.

ACKNOWLEDGMENTS

We would like to thank Dr. Valery Zavorotny and Dr. Mikhail Charnotskii for helpful discussions about statistics of the travel-time fluctuations. This research was partially funded by the U.S. Army Engineer Research and Development Center (ERDC) basic research program. Permission to publish was granted by Director, Cold Regions Research and Engineering Laboratory.

AUTHOR DECLARATION

Conflict of Interest

The authors have no conflicts to disclose.

DATA AVAILABILITY

Data sharing is not applicable to this article as no new data were created or analyzed in this study.

¹B. Chide, P. Blanc-Benon, T. Bertrand, X. Jacob, J. Lasue, R. D. Lorenz, F. Montmessin, N. Murdoch, J. Pla-Garcia, F. Seel, S. Schröder, A. E. Stott, M. de la Torre Juarez, and R. C. Wiens, “An acoustic investigation of the near-surface turbulence on Mars,” *J. Acoust. Soc. Am.* **155**, 420–435 (2024).

²B. Iooss, P. Blanc-Benon, and C. Lhuillier, “Statistical moments of travel times at second order in isotropic and anisotropic random media,” *Waves Random Media* **10**, 381–394 (2000).

- ³S. N. Molodtsov and A. I. Saichev, "Phase fluctuations of a wave in the region of strong fluctuations," *Radiophys. Quantum Electron.* **20**(5), 496–501 (1977).
- ⁴V. E. Ostashev and D. K. Wilson, *Acoustics in Moving Inhomogeneous Media*, 2nd ed. (CRC Press, Boca Raton, FL, 2015), 521 pp.
- ⁵V. E. Ostashev and D. K. Wilson, "Statistical characterization of sound propagation over vertical and slanted paths in a turbulent atmosphere," *Acta Acust.* **104**(4), 571–585 (2018).
- ⁶V. E. Ostashev and D. K. Wilson, "Non-Markov character of the phase fluctuations for sound propagation over relatively small ranges in the turbulent atmosphere," *J. Acoust. Soc. Am.* **145**(6), 3359–3369 (2019).
- ⁷V. E. Ostashev, E. Shabalina, D. K. Wilson, and M. J. Kamrath, "Non-Markov behavior of acoustic phase variance in the atmospheric boundary layer," *Waves Random Complex Media* **33**(5–6), 1266–1281 (2023).
- ⁸A. Petrosyan, B. Galperin, S. E. Larsen, S. R. Lewis, A. Määttänen, P. L. Read, N. Renno, L. P. H. T. Rogberg, H. Savijärvi, T. Siili, A. Spiga, A. Toigo, and L. Vázquez, "The Martian atmospheric boundary layer," *Rev. Geophys.* **49**(3), RG3005, <https://doi.org/10.1029/2010RG000351> (2011).
- ⁹P. L. Read, B. Galperin, S. E. Larsen, S. R. Lewis, A. Maattanen, A. Petrosyan, N. Renno, H. Savijarvi, T. Siili, A. Spiga, A. Toigo, and L. Vazquez, "The Martian planetary boundary layer," in *The Atmosphere and Climate of Mars*, edited by R. M. Haberle, R. T. Clancy, F. Forget, M. D. Smith, and R. W. Zurek (Cambridge University Press, Cambridge, UK, 2017), pp. 172–202.
- ¹⁰V. E. Ostashev and D. K. Wilson, "Strength and wave parameters for sound propagation in random media," *J. Acoust. Soc. Am.* **141**(3), 2079–2092 (2017).
- ¹¹H. Sato, M. C. Fehler, and T. Maeda, *Wave Propagation and Scattering in the Heterogeneous Earth*, 2nd ed. (Springer, Berlin, 2012), 496 pp.
- ¹²S. M. Rytov, Y. A. Kravtsov, and V. I. Tatarskii, *Principles of Statistical Radio Physics. Part 4, Wave Propagation through Random Media* (Springer, Berlin, 1989), 188 pp.
- ¹³A. Ishimaru, *Wave Propagation and Scattering in Random Media* (IEEE, New York, 1997), 572 pp.
- ¹⁴A. D. Wheelon, *Electromagnetic Scintillation. Vol. 1: Geometrical Optics* (Cambridge University Press, New York, 2001).
- ¹⁵A. D. Wheelon, *Electromagnetic Scintillation. Vol. 2: Weak Scattering* (Cambridge University Press, New York, 2003).
- ¹⁶L. C. Andrews and R. L. Phillips, *Laser Beam Propagation through Random Media* (SPIE, Bellingham, WA, 2005), 808 pp.
- ¹⁷V. I. Tatarskii, *The Effects of the Turbulent Atmosphere on Wave Propagation* (Israel Program for Scientific Translation, Jerusalem, 1971).
- ¹⁸S. Shapiro, R. Schwarz, and N. Gold, "The effect of random isotropic inhomogeneities on the phase velocity of seismic waves," *Geophys. J. Int.* **127**, 783–794 (1996).
- ¹⁹Y. Samuelides, "Velocity shift using the Rytov approximation," *J. Acoust. Soc. Am.* **104**, 2596–2603 (1998).
- ²⁰J. L. Codona, D. B. Creamer, S. M. Flatte, R. G. Frehlich, and F. S. Henyey, "Average arrival time of wave pulses through continuous random media," *Phys. Rev. Lett.* **55**(1), 9–12 (1985).
- ²¹V. E. Ostashev, D. K. Wilson, and C. R. Hart, "Influence of ground blocking on the acoustic phase variance in a turbulent atmosphere," *J. Acoust. Soc. Am.* **154**(1), 346–360 (2023).
- ²²V. E. Ostashev, M. J. Kamrath, D. K. Wilson, M. J. White, C. R. Hart, and A. Finn, "Vertical and slanted sound propagation in the near-ground atmosphere: Coherence and distributions," *J. Acoust. Soc. Am.* **150**(4), 3109–3126 (2021).
- ²³M. J. Kamrath, V. E. Ostashev, D. K. Wilson, M. J. White, C. R. Hart, and A. Finn, "Vertical and slanted sound propagation in the near-ground atmosphere: Amplitude and phase fluctuations," *J. Acoust. Soc. Am.* **149**(3), 2055–2071 (2021).
- ²⁴S. Cheinet, M. Cosnefroy, F. Königstein, W. Rickert, M. Christoph, S. L. Collier, A. Dagallier, L. Ehrhardt, V. E. Ostashev, A. Stefanovic, T. Wessling, and D. K. Wilson, "An experimental study on the atmospheric-driven variability of impulse sounds," *J. Acoust. Soc. Am.* **144**(2), 822–840 (2018).
- ²⁵N. Murdoch, A. E. Stott, D. Mimoun, B. Pinot, A. Chatain, A. Spiga, O. Temel, J. P. Garcia, K. Onodera, R. Lorenz, M. Gillier, C. Newman, R. F. Garcia, L. Lange, and D. Banfield, "Investigating diurnal and seasonal turbulence variations of the Martian atmosphere using a spectral approach," *Planet. Sci. J.* **4**, 222 (2023).
- ²⁶D. K. Wilson, "A three-dimensional correlation/spectral model for turbulent velocities in a convective boundary layer," *Boundary-Layer Meteorol.* **85**, 35–52 (1997).
- ²⁷Mars Climate Database version 6.1, available at www-mars.lmd.jussieu.fr (Last viewed August 2, 2024).